

Table of Contents

Figures S1–S15.....	S1-S10
Tables S1–S5.....	S11-S12
References.....	S13

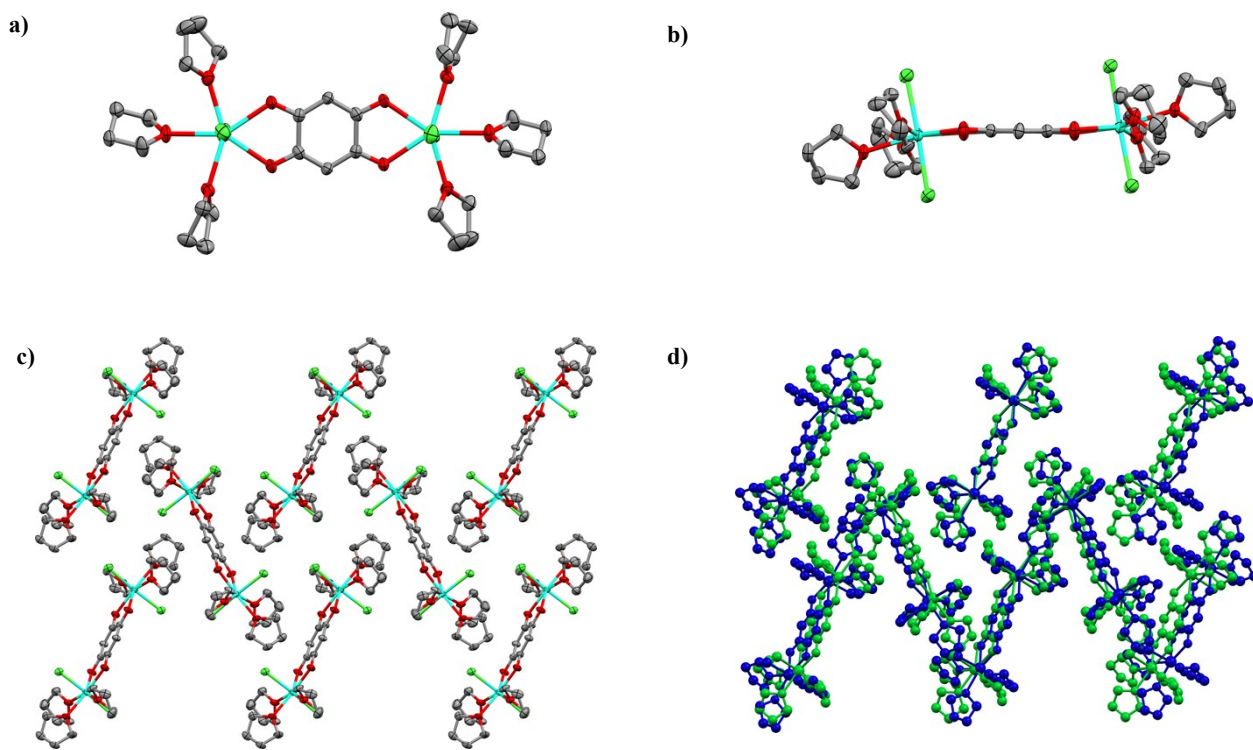


Figure S1 The top (a) and side (b) view of the crystal structure of **2** measured at 120 K. The packing of **2** along *a*-axis (c). The overlay picture of low (120 K, green) and high (293 K, blue) temperature structures along *a*-axis. Thermal ellipsoids are drawn at 50 % probability. Hydrogen atoms are omitted for clarity (black = C; red = O; Green = chlorine; turquoise = dysprosium).

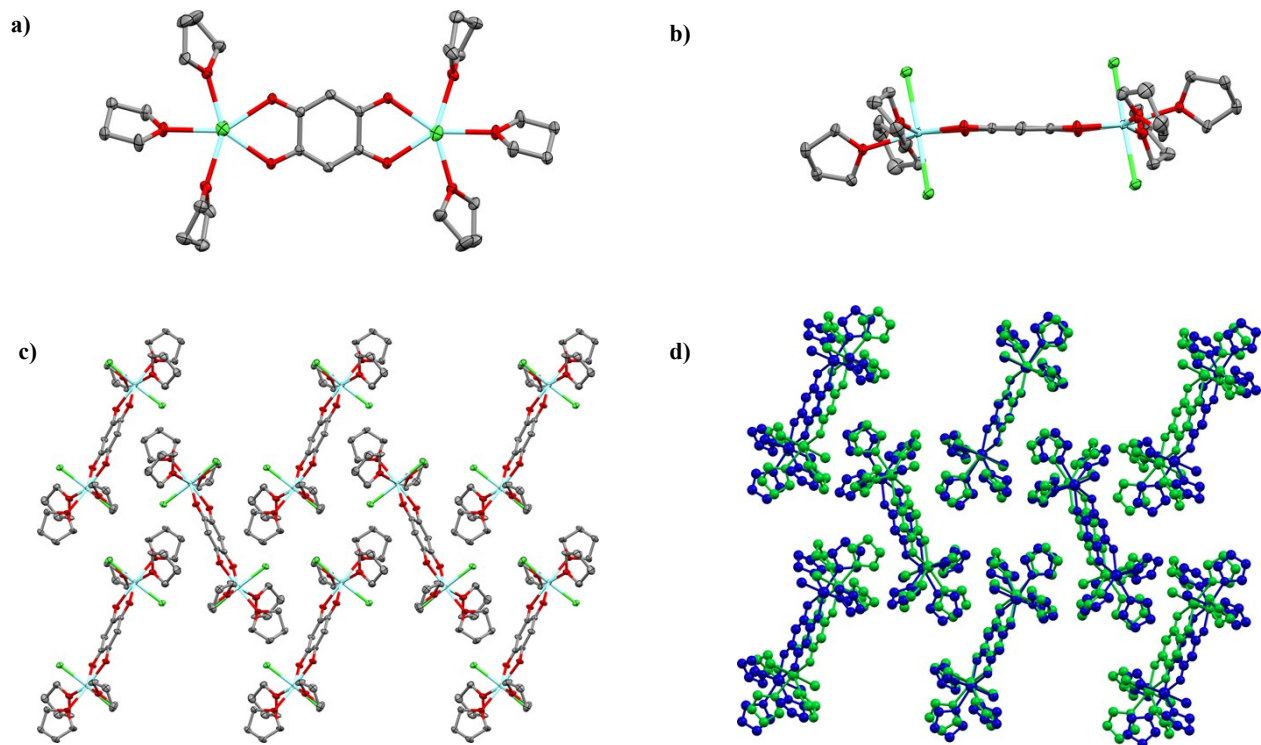


Figure S2 The top (a) and side (b) view of the crystal structure of **1** measured at 120 K. The packing of **1** along *a*-axis (c). The overlay picture of low (120 K, green) and high (293 K, blue) temperature structures. Thermal ellipsoids are drawn at 50 % probability. Hydrogen atoms are omitted for clarity (black = C; red = O; Green = chlorine; light blue = yttrium)

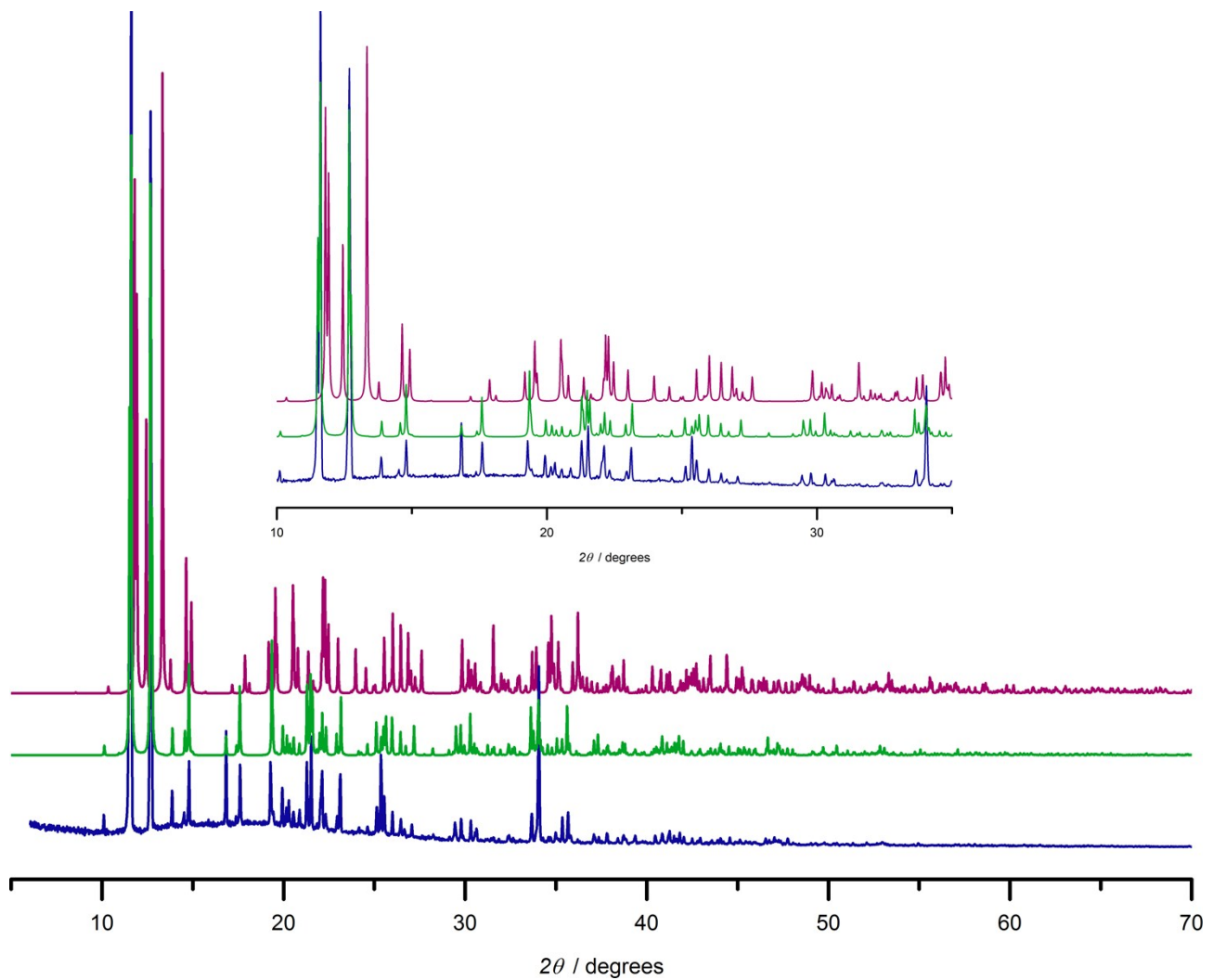


Figure S3 Calculated (red 120 K and green 293 K) and experimental (blue 293 K) powder patterns from 5 to 70 degrees and from 10 to 35 degrees (inset) for **1**.

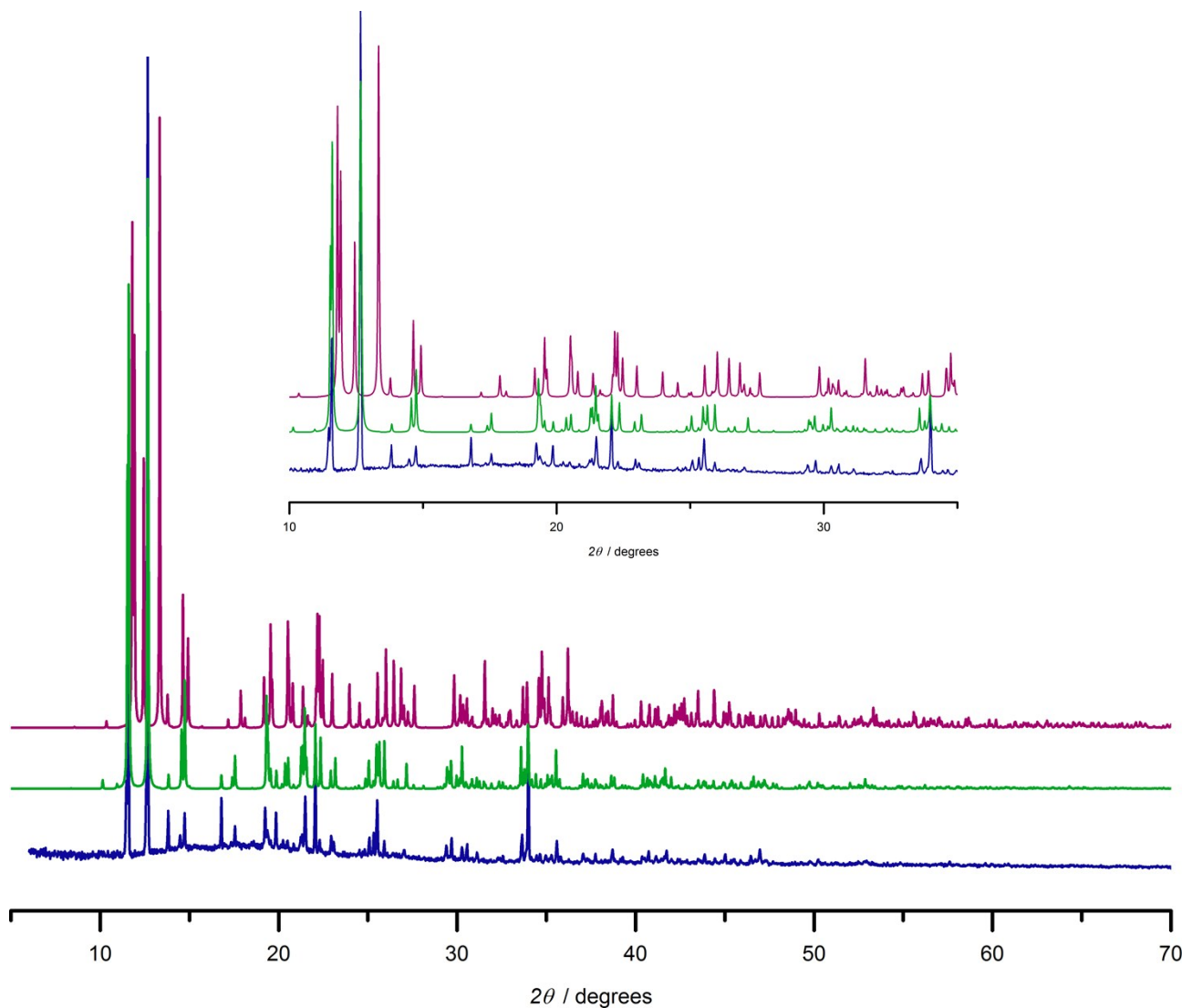


Figure S4 Calculated (red 120 K and green 293 K) and experimental (blue 293 K) powder patterns from 5 to 70 degrees and from 10 to 35 degrees (inset) for **2**.

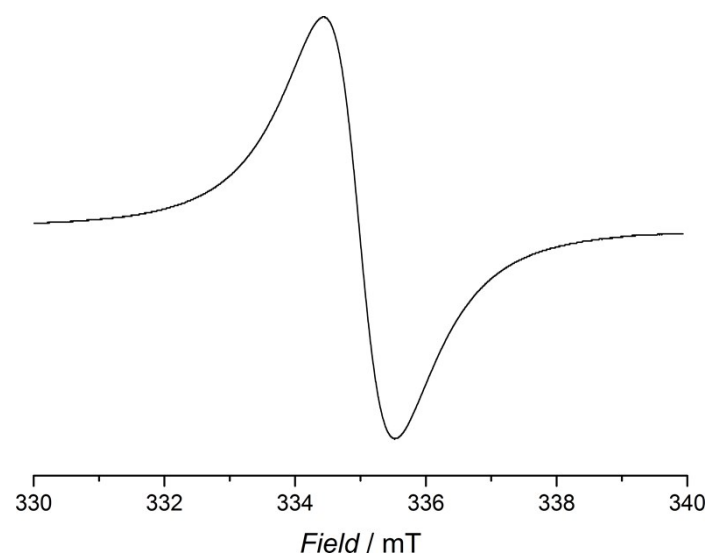


Figure S5 Powder X-band EPR spectrum of **1[•]** at 293 K (mod. amp. = 0.2 G, $\text{lw} = 1.09 \text{ mT}$, $\text{g}_{\text{iso}} = 2.003 \text{ G}$).

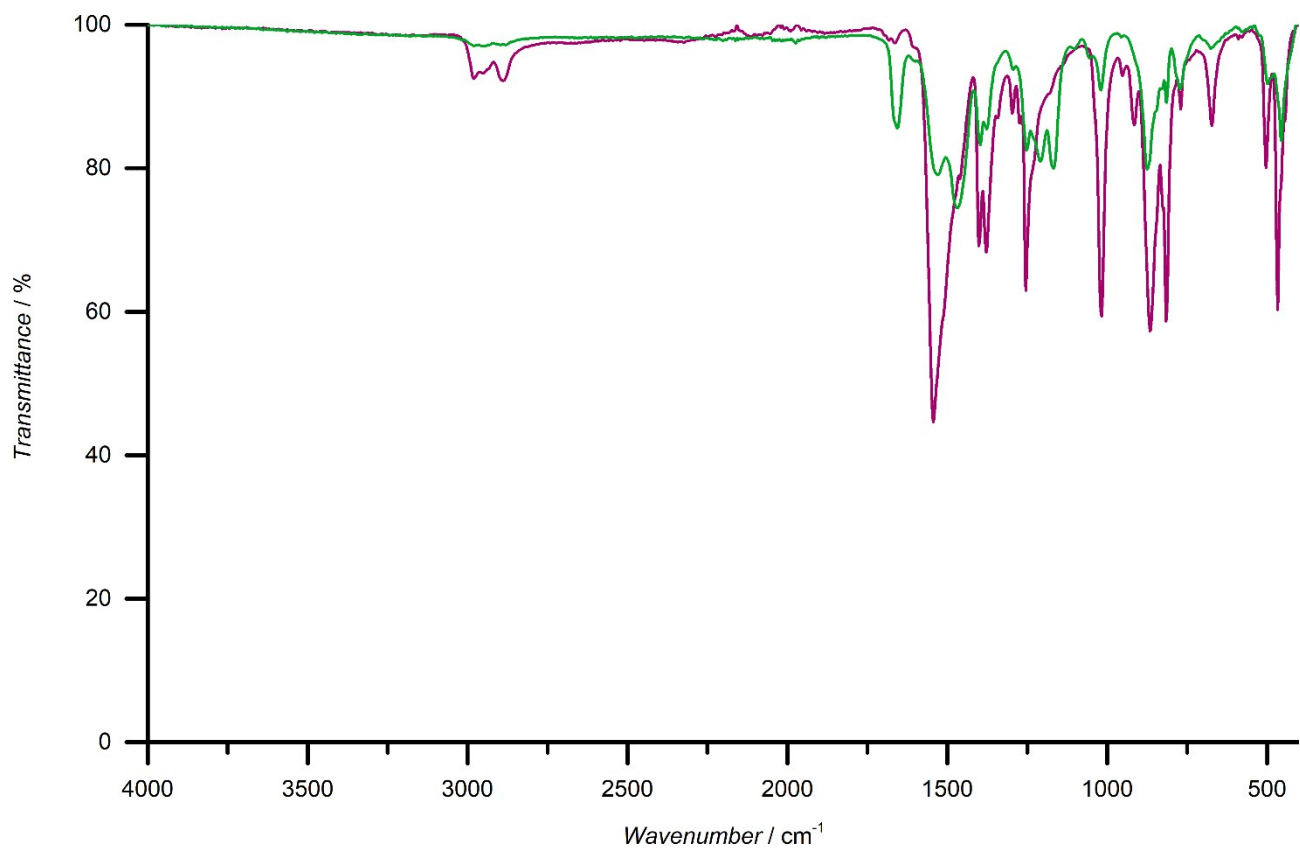


Figure S6 IR spectrum of **1** (red) and **1^{•-}** (green).

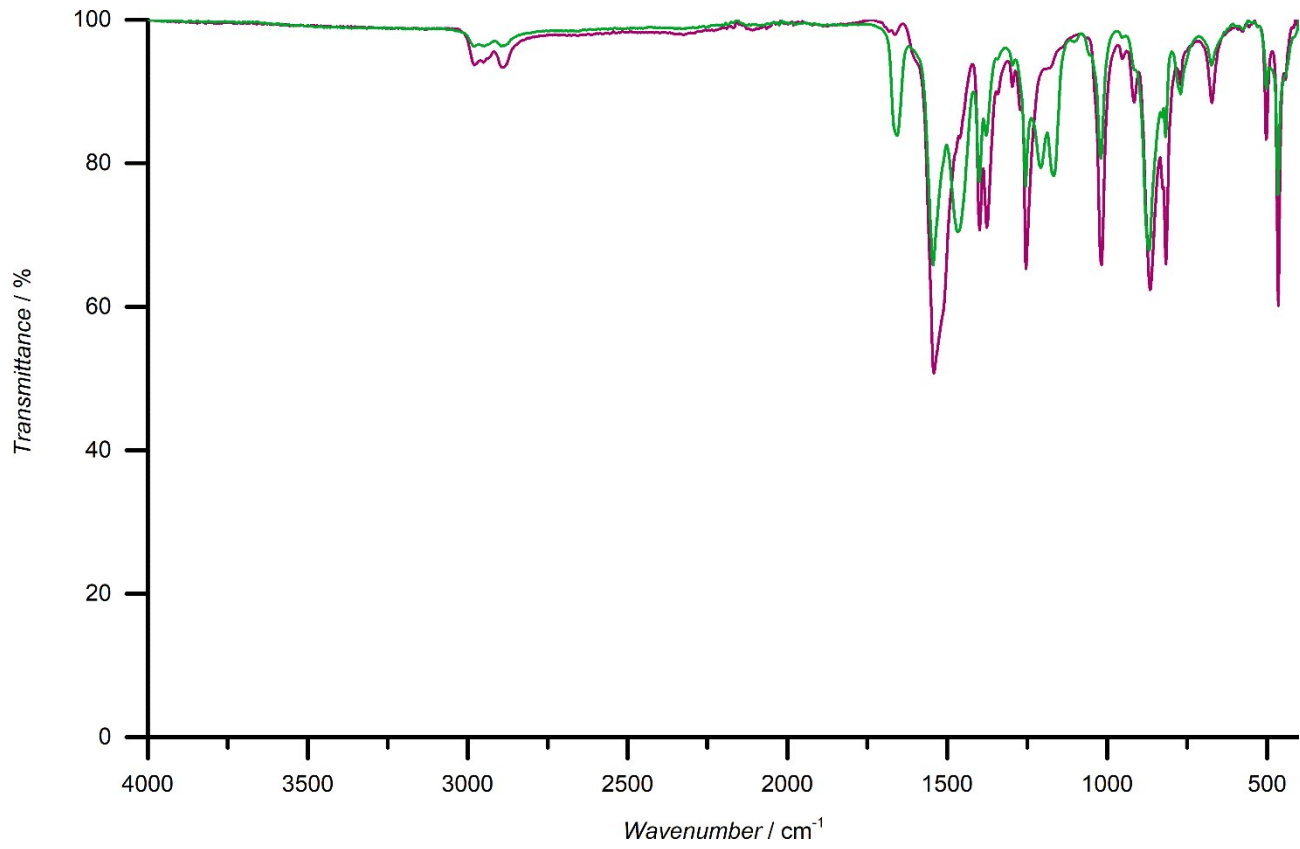


Figure S7 IR spectrum of **2** (red) and **2^{•-}** (green).

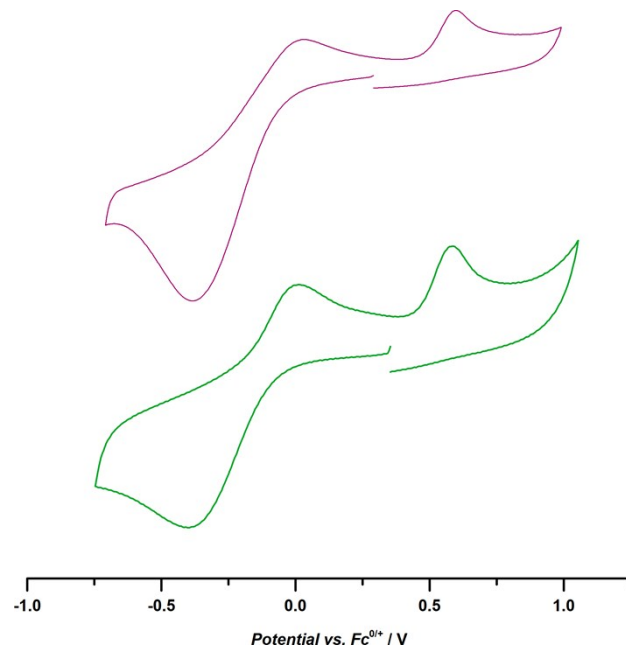


Figure S8 Cyclic voltammograms showing the observed reduction and oxidation processes for **1** (red) and **2** (green) in THF solutions containing 0.1 M $[(\text{n-Bu})_4\text{N}]^+[\text{PF}_6]^-$ at Pt electrode with scan rate 0.2 V s⁻¹. The $E^{1/2}$ potentials as well as peak potentials and currents are given in Table S3.

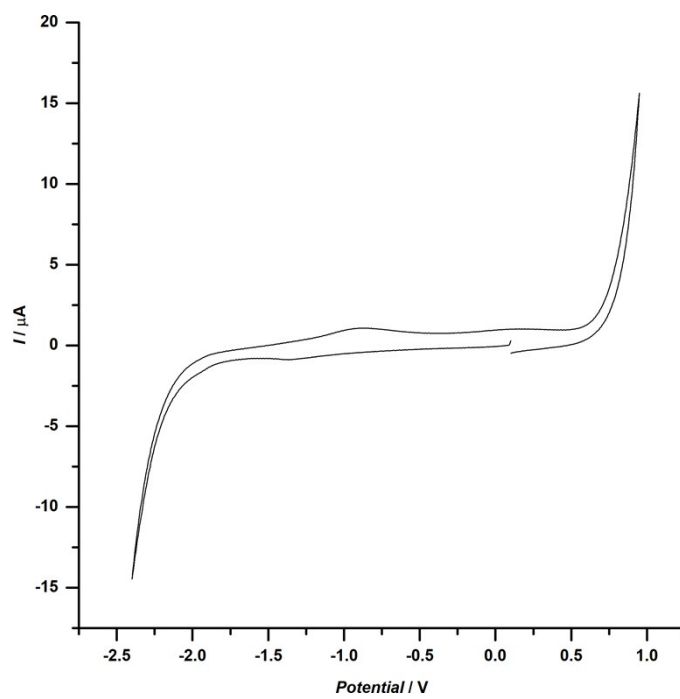


Figure S9 Cyclic voltammogram showing a potential window in THF solutions containing 0.1 M $[(\text{n-Bu})_4\text{N}]^+[\text{PF}_6]^-$ at Pt electrode with scan rate 0.2 V s⁻¹.

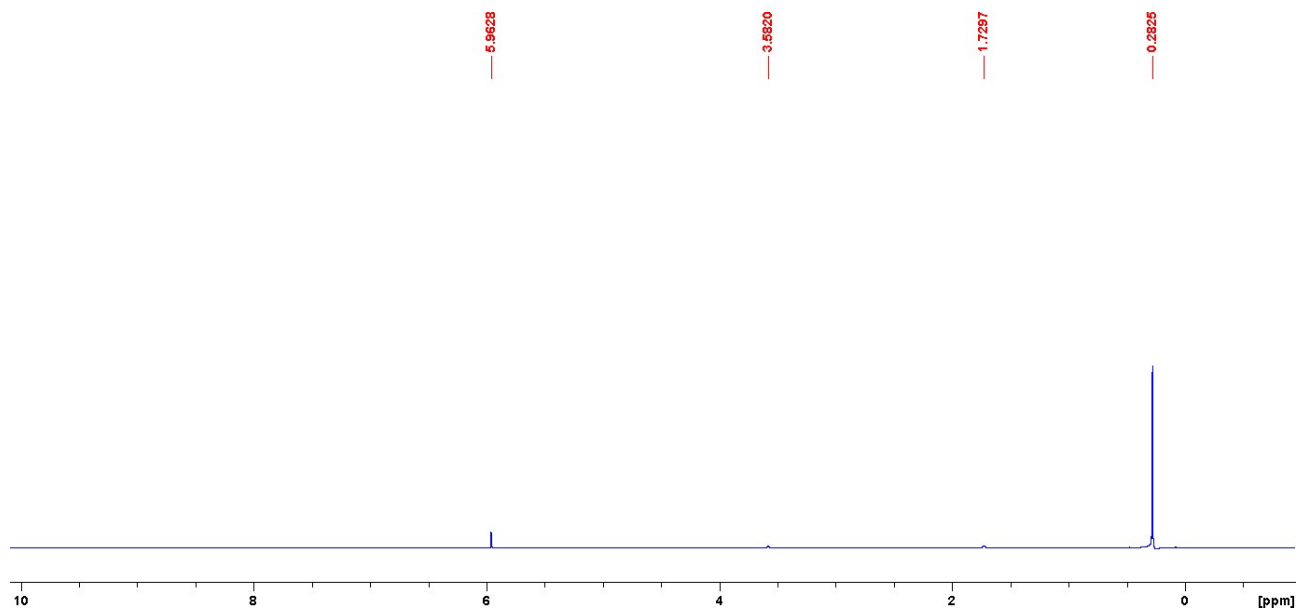


Figure S10 ¹H NMR spectrum of **3** in THF-d₈.



Figure S11 The crystals structure of **3** measured at 120 K. Hydrogen atoms are omitted for clarity and thermal ellipsoids are drawn at 50 % probability (black = C; red = O; yellow = Si).¹

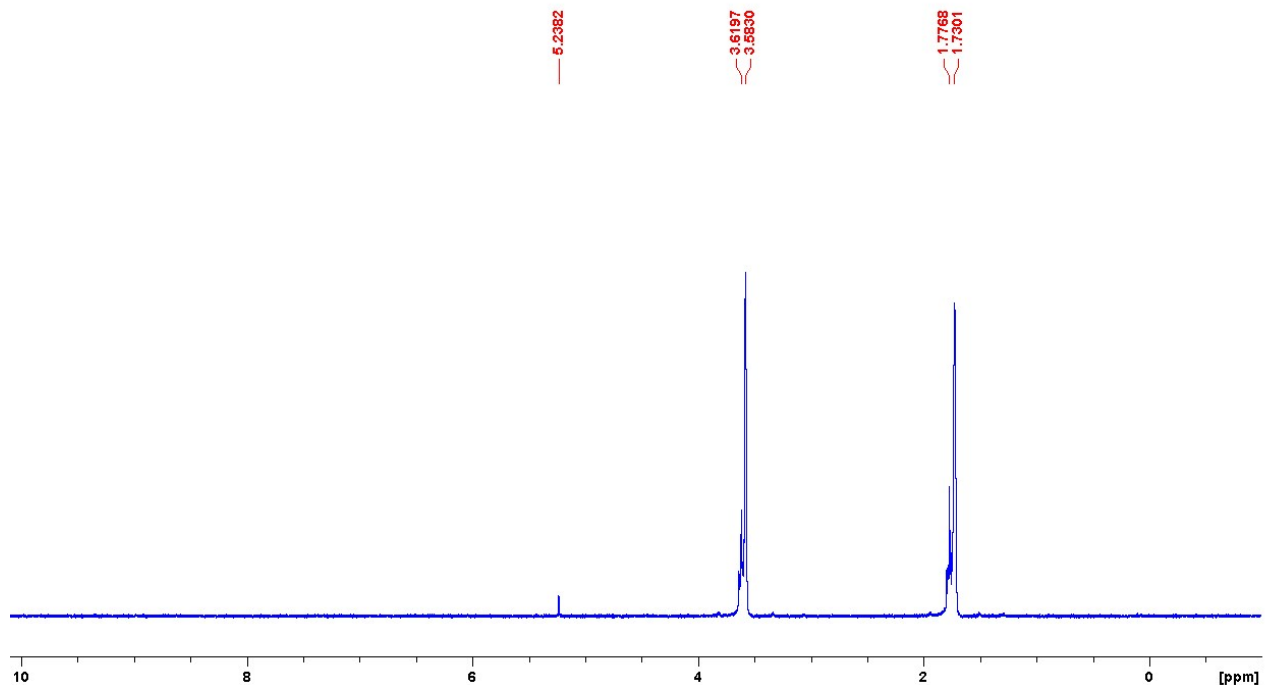


Figure S12 ^1H NMR spectrum of **1** in THF-d_8 .

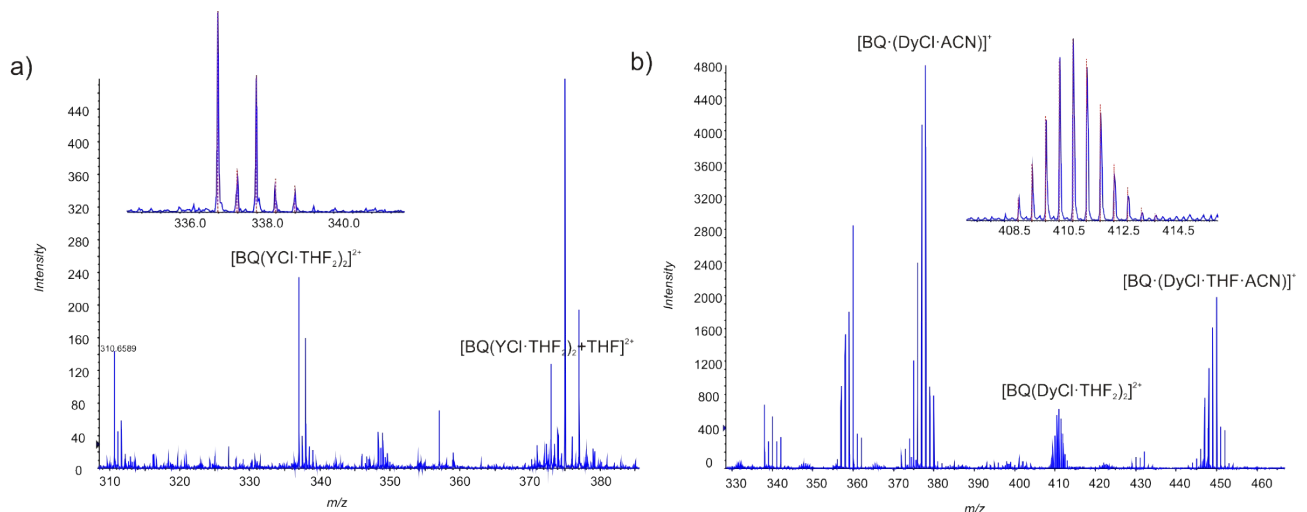


Figure S13 ESI-MS spectra of complexes a) 1 and b) 2. Insets show the experimental isotopic distribution for the complexes and their comparison to theoretical pattern (red dotted line) calculated on basis of natural abundances for elements.

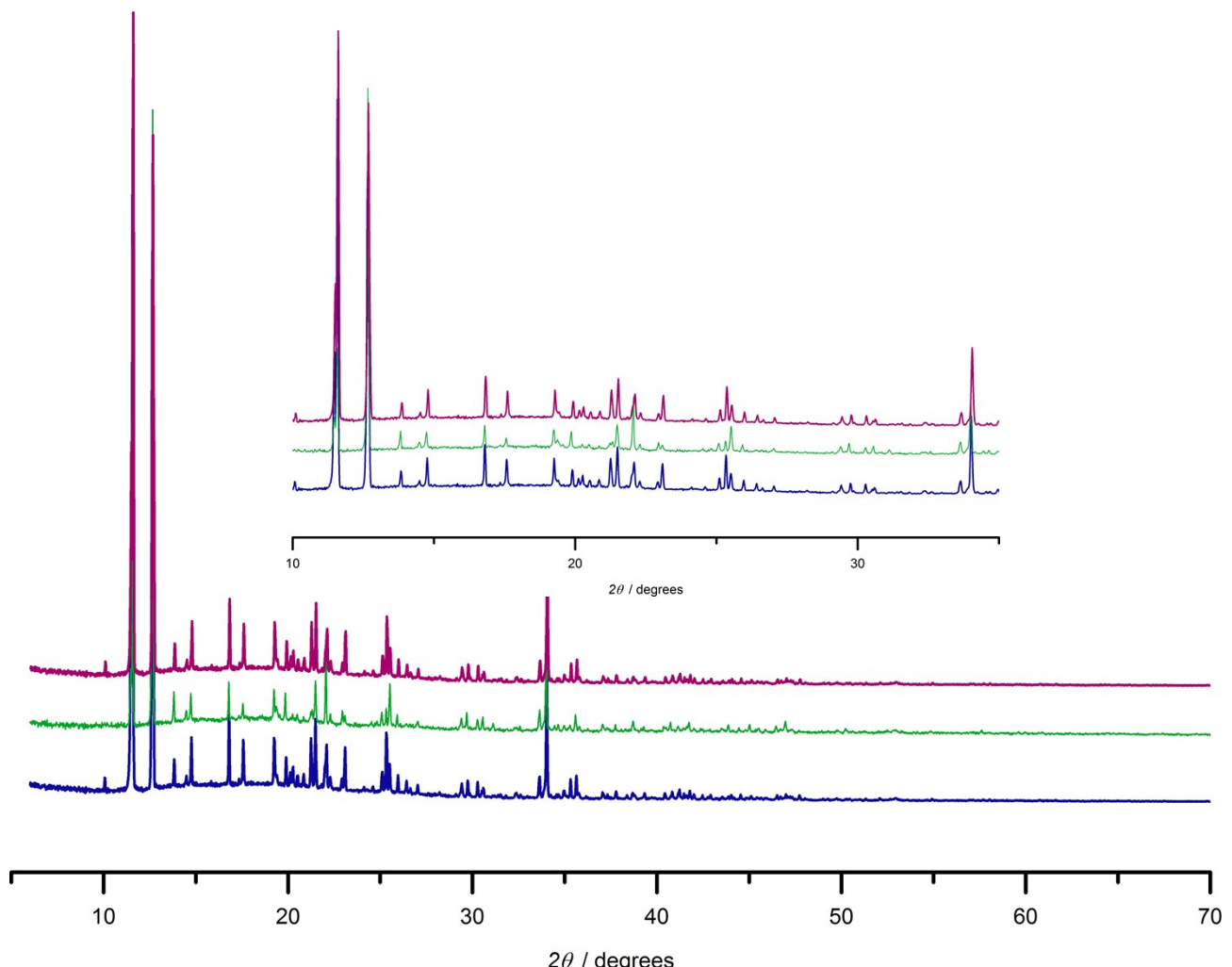


Figure S14 Experimental powder patterns 5 to 70 degrees and from 10 to 35 degrees (inset) for **1** (red), **2** (green) and doped sample **Dy@1** (blue) at 293 K.

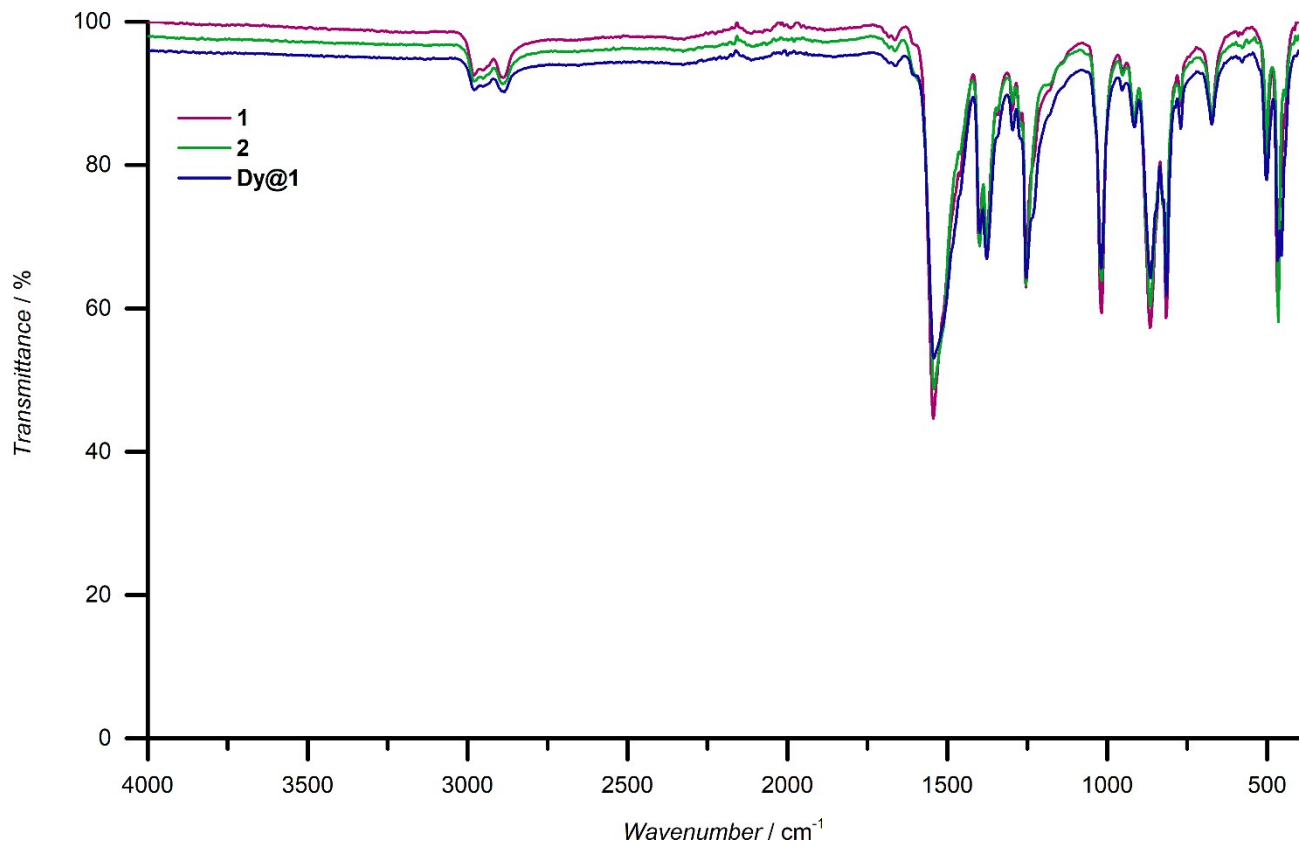


Figure S15 IR spectra of **1** (red), **2** (green), **Dy@1** (blue). The Y-axes of **2** and **Dy@1** are slightly displaced for the clarity.

Table S1 Selected bond lengths and angles for **1** and **2**.

1				2			
Bond (Å)	Angle (°)		Bond (Å)	Angle (°)			
Y1-Cl1	2.5999(7)	Cl1-Y1-Cl2	176.26(2)	Dy1-Cl1	2.603(2)	Cl1-Dy1-Cl2	175.87(8)
Y1-Cl2	2.5819(7)	Cl1-Y1-O1	84.74(5)	Dy1-Cl2	2.587(2)	Cl1-Dy1-O1	84.90(17)
Y1-O1	2.3301(17)	Cl1-Y1-O2	88.42(5)	Dy1-O1	2.338(6)	Cl1-Dy1-O2	88.93(17)
Y1-O2	2.3124(17)	Cl1-Y1-O3	89.73(5)	Dy1-O2	2.329(6)	Cl1-Dy1-O3	89.60(18)
Y1-O3	2.375(2)	Cl1-Y1-O4	82.15(5)	Dy1-O3	2.388(6)	Cl1-Dy1-O4	81.93(17)
Y1-O4	2.4097(18)	Cl1-Y1-O5	97.04(5)	Dy1-O4	2.427(6)	Cl1-Dy1-O5	97.53(16)
Y1-O5	2.3652(19)	Cl2-Y1-O1	98.59(5)	Dy1-O5	2.393(6)	Cl2-Dy1-O1	98.76(17)
C1-O1	1.265(3)	Cl2-Y1-O2	91.24(5)	C1-O1	1.272(10)	Cl2-Dy1-O2	90.68(17)
C2-O2	1.259(3)	Cl2-Y1-O3	86.61(5)	C2-O2	1.273(10)	Cl2-Dy1-O3	86.37(18)
C1-C2	1.528(4)	Cl2-Y1-O4	96.04(5)	C1-C2	1.524(12)	Cl2-Dy1-O4	96.08(17)
C1-C3	1.389(4)	Cl2-Y1-O5	85.60(5)	C1-C3	1.383(12)	Cl2-Dy1-O5	85.39(15)

Table S2 Observed intermolecular interactions along with their range in the crystal structures of **1** and **2**.

	H···H	C···H	O···H	Cl···H
1	2.258-2.392	2.834	2.645	2.885-2.939
2	2.226-2.366	-	-	-

Table S3 Measured peak potentials and currents as well as $E^{1/2}$ values for **1** and **2**.

Complex	Reduction				Oxidation		
	E^{pc} / V	E^{pa} / V	$E^{1/2} / \text{V}$	$I^c / \mu\text{A}$	$I^a / \mu\text{A}$	E^{pa} / V	
1	-0.386	-0.035	-0.211	25.382	10.588	0.598	6.303
2	-0.397	-0.014	-0.206	5.503	2.199	0.586	1.975

Table S4 *Ab initio* values of the energies and the principal components of the **g** tensors in the eight lowest Kramers doublets (KD) corresponding to the crystal field split components of the ${}^6\text{H}_{15/2}$ multiplet of the Dy³⁺ ions in **2**.

KD	E / cm^{-1}	g_x	g_y	g_z
1	0	0.252	0.817	18.604
2	44	0.206	0.300	19.359
3	74	2.500	4.525	11.653
4	132	8.008	5.110	0.185
5	196	3.068	4.124	11.027
6	251	0.075	1.352	14.788
7	288	0.985	2.392	12.182
8	306	0.842	2.359	14.483

Table S5 Crystal data and structural refinement for **1** and **2** measured at 120 K and 293 K.

	1 / 120K	1 / 293K	2 / 120K	2 / 293K	3 / 120 K
CCDC ref. code	1557623	-	1557624	-	1557625
Formula	C ₃₀ H ₅₀ Cl ₄ O ₁₀ Y ₂	C ₃₀ H ₅₀ Cl ₄ O ₁₀ Y ₂	C ₃₀ H ₅₀ Cl ₄ O ₁₀ Dy ₂	C ₃₀ H ₅₀ Cl ₄ O ₁₀ Dy ₂	C ₁₂ H ₂₀ O ₄ Si ₂
FW	890.32	890.32	1037.50	1037.50	284.46
Crystal system	monoclinic	monoclinic	monoclinic	monoclinic	monoclinic
Space group	<i>P</i> 2 ₁ / <i>n</i>	<i>P</i> 2 ₁ / <i>n</i>	<i>P</i> 2 ₁ / <i>n</i>	<i>P</i> 2 ₁ / <i>n</i>	<i>P</i> 2 ₁ / <i>c</i>
<i>a</i> /Å	9.0004(2)	14.6798(17)	9.0173(5)	14.725(3)	6.38820(16)
<i>b</i> /Å	14.8832(3)	16.154(2)	14.9995(9)	16.151(2)	9.9721(3)
<i>c</i> /Å	14.8047(3)	9.1377(11)	14.8171(8)	9.1228(14)	11.9758(3)
<i>α</i> /°	90	90	90	90	90
<i>β</i> /°	106.160(2)	109.106(11)	106.402(6)	108.879(17)	100.550(3)
<i>γ</i> /°	90	90	90	90	90
<i>V</i> /Å ³	1904.80(7)	2047.5(5)	1922.5(2)	2052.9(6)	750.01(3)
<i>Z</i>	2	2	2	2	2
Crystal size/mm ³	0.15 × 0.10 × 0.06	0.11 × 0.06 × 0.05	0.15 × 0.07 × 0.07	0.11 × 0.07 × 0.02	0.54 × 0.08 × 0.08
2θ range/°	10.392 to 135.962	8.402 to 133.994	8.57 to 137.964	8.382 to 133.972	11.63 to 139.988
Reflections collected	6301	6386	13827	6707	2455
Independent reflections, <i>R</i> _{int}	3443, 0.0325	3528, 0.0437	3572, 0.0465	3620, 0.1243	1415, 0.0169
Completeness/%	99.5	97.1	99.9	99.2	99.5
Data/restraints/parameters	3443/0/208	3528/0/208	3572/0/208	3620/396/104	1415/0/85
Goodness-of-fit on <i>F</i> ²	1.037	1.140	1.180	0.980	1.036
Final <i>R</i> indices [<i>I</i> >2σ(<i>I</i>)]	<i>R</i> ₁ = 0.0296 <i>wR</i> ₂ = 0.0717	<i>R</i> ₁ = 0.0589 <i>wR</i> ₂ = 0.1539	<i>R</i> ₁ = 0.0531 <i>wR</i> ₂ = 0.1496	<i>R</i> ₁ = 0.1890 <i>wR</i> ₂ = 0.4197	<i>R</i> ₁ = 0.0314 <i>wR</i> ₂ = 0.0814
<i>R</i> indices (all data)	<i>R</i> ₁ = 0.0354 <i>wR</i> ₂ = 0.0764	<i>R</i> ₁ = 0.1106 <i>wR</i> ₂ = 0.2460	<i>R</i> ₁ = 0.0584 <i>wR</i> ₂ = 0.1524	<i>R</i> ₁ = 0.2883 <i>wR</i> ₂ = 0.5371	<i>R</i> ₁ = 0.0332 <i>wR</i> ₂ = 0.0834
Largest diff. peak/hole / e Å ⁻³	0.62/-0.39	0.78/-1.49	1.73/-1.08	0.78/-2.64	0.28/-0.27

Table S6 HR-ESI-MS results for the complexes observed. Experimental and theoretical m/z values, charge states and molecular formulas.

ion	charge (+)	composition	<i>m/z</i> _{theor}	<i>m/z</i> _{exp}	MW _{exp} (Da)	MW _{theor} (Da)	Δ _{<i>m/z</i>}
[BQ(YCl·THF ₂) ₂] ²⁺	2	C ₂₂ H ₃₄ O ₈ Cl ₂ Y ₂	336.9868	336.9858	673.9716	673.9736	0.001
[BQ(YCl·THF ₂) ₂ +THF] ²⁺	2	C ₂₆ H ₄₂ O ₉ Cl ₂ Y ₂	373.0156	373.0155	746.031	746.0312	0.0001
[BQ(DyCl ₃ ·THF ₂) ₂] ²⁺	2	C ₂₂ H ₃₄ O ₈ Cl ₂ Dy ₂	411.0087	411.0336	822.0672	822.0174	-0.025
[BQ(DyCl ₃ ·THF·ACN)] ⁺	1	C ₁₂ H ₁₃ O ₅ NClDy	449.9762	450.0671	450.0671	449.9762	-0.091
[BQ(DyCl ₃ ·ACN)] ⁺	1	C ₈ H ₄ O ₄ NClDy	377.9187	377.9975	377.9975	377.9187	-0.079

References

1. The crystal structure of **3** has been reported without synthetic details in private communication before: J. Wagler, E. Kroke and K. Krupinski, *CSD Communication (Private Communication)*, Refcode = GOFTAY.